Translational Oncology 16 (2022) 101316

Contents lists available at ScienceDirect

Translational Oncology

journal homepage: www.elsevier.com/locate/tranon

Original Research

EZH2 targeting to improve the sensitivity of acquired radio-resistance bladder cancer cells

Xiangyan Zhang [1], Xiangli Ma [1], Quanxin Wang, Zhaolu Kong [*]

The Institute of Radiation Medicine, Fudan University, 2094 Xietu Road, Shanghai 200032, P.R. China

ARTICLE INFO

Keywords:
Bladder cancer
Acquired radio-resistance
EZH2
Radiosensitivity
Autophagy

ABSTRACT

Among the many treatments for Bladder cancer (BCa) patients, radiotherapy is an effective way to preserve the bladder. However, as the frequency of irradiation increases, the tumor cells appear "acquired radio-resistance" (ARR) and loss the sensitivity to radiotherapy. To explore the molecular mechanism of ARR, two BCa cell lines, 5637 and T24, were enrolled here and their ARR counterparts, 5637R and T24R, were obtained by exposure to γ-ray of 2 Gy for 30 times. Compared to parental cells, ARR cells have significantly enhanced stem cell-like phenotype, robust DNA damage repair capabilities and elevated expression of zeste homolog 2 (EZH2). Decreasing EZH2 expression, both parental and ARR cells exhibited reduced abilities of forming microsphere and repairing DNA damage, but enhanced cells radio-sensitivity and intracellular autophagy compared to untreated cells. Down-regulation the expression of EZH2 induced an increasing of both LC3 and P62 in parental cells, while in ARR cells, only LC3 increased upon EZH2 reduction. On the other hand, UNC1999 treatment caused the increasing of LC3B and P62 in all cells, suggested that siEZH2 and UNC1999 affect ARR cells autophagy through different mechanisms. In vivo study showed that pre-treated with UNC1999 greatly enhanced T24R cells sensitivity to IR, and knocking down the expression of EZH2 significantly suppressed the tumor growth. Combined with bioinformatics data analysis, we speculate that EZH2 is an important biomolecule linking the diagnosis, radiotherapy and prognosis of BCa. EZH2 targeted therapy may be an effective way to overcome ARR of BCa, and is worthy of in-depth study.

Introduction

Bladder cancer (BCa) is the tenth most common cancer in the world and the most common malignant tumor of the urinary system. Its incidence is steadily increasing, especially in developed countries [1, 2]. According to the latest report of International Agency for Research on Cancer (IARC), there are 570,000 new cases of BCa worldwide and 210,000 deaths in 2020 [3]. Transitional cell carcinoma accounts for more than 80% of all BCa, and is divided into non-muscle-invasive bladder cancer (NMIBC) and muscle-invasive bladder cancer (MIBC) with different prognosis. In terms of disease management, transurethral resection and radical cystectomy with extended lymphadenectomy are considered the initial treatment of choice for NMIBC and MIBC, respectively. Actually, a considerable number of patients with BCa are elderly or frailer, and they are ineligibility for surgical treatment. Therefore, bladder-preserving based radiotherapy is recommended as an alternative to surgery for the treatment of BCa. Moreover, radiation therapy is also suitable for BCa patients who have recurred after surgery [4]. In clinic, fractionated irradiation(FI) is commonly adopted to avoid and reduce the damage effect of radiation on normal tissues. For BCa treatment, the total dose is 64 Gy, divided into 32 irradiations for 6.5 weeks, or the total dose is 55 Gy, divided into 20 times lasting 4 weeks [5]. However, the occurrence of acquired radio-resistance (ARR) caused poor efficacy of BCa radiotherapy [6]. At present, the molecular changes caused by FI during tumor radiotherapy and the mechanism of ARR are still unclear.

Cancer stem cells (CSCs) have the characteristics of self-renewal, asymmetric division and multidirectional differentiation. Based on their strong DNA damage repair capabilities and fast self-renewal abilities, CSC exhibit strong resistance to radiotherapy and chemotherapy through abnormal expression of membrane transporters and anti-apoptotic proteins [7]. Bladder cancer stem cells (BCSCs) are BCa cells

Abbreviations: EZH2, Enhancer of Zeste Homolog 2; ARR, Aquired Radio-Resistance; BCa, Bladder Cancer.

* Corresponding author.
E-mail address: kongzhaolu@fudan.edu.cn (Z. Kong).

[1] Authors contributed equally to this work.

https://doi.org/10.1016/j.tranon.2021.101316
Received 1 October 2021; Received in revised form 11 December 2021; Accepted 14 December 2021

with multi-differentiation potential. Their stemness is regulated by genetics and epigenetics and considered to be the initiation of BCa. BCSCs are resistant to a variety of treatments and are the main factor for the recurrence of BCa. Therefore, they play an important role in the study of the pathogenesis, diagnosis and treatment of BCa.

Enhancer of zeste homolog 2 (EZH2) encodes a histone methyltransferase, which is the catalytic core protein of the polycomb repressor complex 2 (PRC2). PRC2 is well known for initiating target gene silencing by promoting H3K27 trimethylation, which is catalyzed by EZH2. Previous research has shown that the EZH2 is involved in the cell proliferation, invasion, apoptosis, angiogenesis, and metastasis of cancer progression [8, 9]. Herein, we observed that higher levels of EZH2 expression in BCa patients are associated with poor prognosis. Furthermore, we demonstrate that EZH2 promotes the process of radiation-induced stem cell-like transformation and radio-resistance through DNA damage repair, and autophagy. These results indicate that EZH2 might be a potential therapeutic target for preventing clinical BCa radiotherapy resistance and progression.

Methods and materials

Cell culture

Three human-derived tumor cell lines, 5637 and T24 (bladder cancer), MDA-MB-231 (breast cancer), were maintained in Dulbecco's modified Eagle's medium (DMEM, high glucose, Invitrogen, Thermo Fisher Scientific, Inc., Waltham, MA, USA) containing 10% fetal bovine serum (FBS, Invitrogen), 100 U/ml penicillin and 100 U/ml streptomycin (Sigma-Aldrich, Merck KGaA, Darmstadt, Germany) under a humidified atmosphere of 5% carbon dioxide at 37℃.

Irradiation(IR) and ARR cell models

Cells were irradiated at room temperature in ambient air using a ^{137}Cs source (γ-ray, MDS Nordion, Toronto, Canada) at a dose rate of 0.77 Gy/min. In order to mimic the clinical radiotherapy treatment, the parental cell lines, 5637, T24 and MDA-MB-231 were exposed to γ-rays at 2 Gy for a continuous 5 days followed by a 2-day interval, with a cumulative dose of 60Gy. The surviving cells after 1 month of culture were collected and named 5637R, T24R and MDA-MB-231R, respectively. The ARR phenotype of above cells were confirmed every three months with colony formation assay. In vivo experiments, nude mice were anesthetized, and subcutaneous tumors were irradiated with 4 Gy X-ray (X-RAD 320, PXI Inc., North Branford) every other day, and the cumulative dose was 12 Gy for a total of 3 irradiations.

Colony formation assay (CFA)

Two hours post ionizing radiation (IR), cells under different treatment and control cells were trypsinized to a single-cell suspension. Then cells were counted and seeded into 6-cm dishes. After 2 weeks of incubation, the colonies were fixed with 100% methyl alcohol at room temperature for 30 min, stained with 0.2% crystal violet for 30 min at room temperature (RT), cleaned with water, counted after sufficiently dried and the surviving fraction was calculated.

Quantitative real-time polymerase chain reaction (qRT-PCR)

Total RNA was extracted and analyzed as described formerly [10]. Total RNA from BCa cells were extracted using an RNA extraction kit (Tiangen Biotech Co., Ltd., Beijing, China). RNA was reverse transcribed into cDNA using cDNA synthesis kit (TOYOBO Co., Ltd, Shanghai, China). qPCR was subsequently performed with SYBR Green RT-PCR reagents (BIOER, Hangzhou, China) under the following thermocycling conditions: 95°C for 5 min, followed by 40 cycles of 95°C for 30 sec and 65°C for 45 sec. The primers of target genes designed by GenScript (Nanjing, Jiangsu, China). Primers were: EZH2, 5'-CTAGGGAGTGTTCGGTGACCA-3'(F) and 5'-ATTCTGCTGTAGGGGAGACCAAG-3'(R); GAPDH,5'-GAGTCAACGGA

TTTGGTCG-3' (F) and 5'-CGGAAGATGGTGATGGGATT-3' (R). Each sample was examined in triplicate and the amount of product was normalized relative to that of GAPDH. ΔΔCt method was applied to calculate the gene expression.

Western blot analysis (WB)

Cellular proteins were extracted with M-PER™ protein extraction kit (Thermo Fisher Scientific, cat. No. 78501). Proteins were quantified (BCA assay kit; cat. No. 23227; Thermo Fisher Scientific) and 50 μg total proteins were loaded on 10% SDS-PAGE gels. Proteins were then fractionated and transferred to polyvinylidene difluoride (PVDF) membranes (0.45 μm, Merck KGaA), blocked with 5% bovine serum albumin (BSA, AR2440, Sangon Biotech Co., Shanghai, China) for 1 h at RT. Subsequently, the membranes were incubated with primary antibodies at 4℃ overnight, and then incubated with secondary antibodies, horseradish peroxidase-conjugated secondary antibodies against mouse or rabbit (1:1000, Beyotime Institute of Biotechnology, Haimen, China) for 1 hour at RT. Finally, the bands were visualized with the ChemiDoc XRS system (Bio-Rad Laboratories, Hercules, CA, USA). Primary antibodies: anti-EZH2, anti-LC3B, anti-Bax, anti-P62, anti-Bcl-2 (1:1000, HuaAn Biotechnology, Hangzhou, China) and anti-GADPH (1:1000; Hangzhou Goodhere Biotechnology).

RNA interference (RNAi)

5×10^5 cells were seeded into 6-cm dishes, and transfection was performed at 60%-70% confluence. Transient inhibition of human EZH2 were carried out by co-transfection with 20nM siRNA (siEZH2, 5′-GACACCCGGUGGGACUCAGAAG-3′) and Lipofectamine 2000 (Invitrogen) according to the manufacturer's instructions. Cells treated with siCon (5′-CT GGACTTCCAGAAGAACA-3′) as control. The medium was replaced 8h later and subsequent experiments were performed after 24h. All siRNA oligonucleotides were synthesized by Genepharma (Shanghai, China).

Sphere formation assay

Cells were trypsinized and washed in DMEM. 2.0×10^5 cells were seeded in ultra-low attachment surface 6-well plate (Corning, Inc., NY, USA) and maintained in the serum-free medium (SFM) supplemented with 20 ng/ml EGF, 20 ng/ml bFGF and 2% B27 (Invitrogen). Cell spheres were imaged by the microscope in five independent fields and spheres with diameters greater than 50 μm were counted after 3-6 days.

Soft agar colony anchoring assay

Low melting point agarose (Sigma-Aldrich) was first dissolved in ultrapure water (concentration, 1.2% and 0.8%). Then prepare the bottom matrix: 2 × DMEM, which contains 2% PS and 30% FBS, were mixed with 1.2% agarose solution at a 1:1 ratio. 3 ml of the mixture was added to 6-cm dishes, cooled and solidified in an incubator. Next, cells were suspended in 3ml medium (2 × DMEM: 0.8% agar solution, 1:1) and move to dishes. After the upper layer of agarose fully solidified, incubated at 37℃ for two weeks. Cells were stained with 0.2% crystal violet (Sangon Biotech Co., Ltd.) for 15-30 min at RT. Finally, the colonies were photographed and counted.

Tumor xenograft in nude mice

The male BALB/c nude mice (age 35-42 days; weight 22-25 g) were purchased from Shanghai SLAC Laboratory Animal Co., Ltd in China. Experimental animals were housed in 24℃, 50-70% humidity, and light /

dark cycle (12h: 12h), and were free to obtain food and water. For generation of xenografts, 5×10^6 tumor cells were injected into the right flank of each mouse. After tumors were measurable, tumor-bearing mice with T24R cells were grouped randomized, untreated control, radiation alone (4 Gy), UNC1999 alone (50mg/kg, every other day, 3 times), and radiation + UNC1999. Tumor sizes were measured and the tumor volume was calculated by following formula: $V=\pi \bullet L \bullet W^2/6$. Mice were sacrificed 13 days after transplantation, and the tumor weight was measured. Then, all tumors were collected for subsequent analysis. All experiments were approved by the Committee for Ethical Use of Experimental Animals at Fudan University (approval no. 201802144S; Shanghai, China) and were compliant with the Guide for the Care and Use of Laboratory Animals.

Immunocytochemical analysis (ICC)

Cells were planted on poly-lysine coated cover slips and exposed to a total radiation dose of 2 Gy. Fix the cells with 4% paraformaldehyde at different time points post-IR. cells were blocked with 5% BSA and stained with rabbit primary antibodies. Alexa Fluor 555 labeled donkey anti-rabbit IgG (1:200) was used as the secondary antibody. Finally, the coverslips were mounted with mounting medium containing 4′,6-diamidino-2-phenylindole (DAPI) and examined with a fluorescence microscope (Olympus Corporation, Tokyo, Japan).

Statistical analysis

The results are presented as the means ± standard errors of the means (SEM) of three independent experiments. Statistical analyses were performed using an unpaired Student's t-test. Statistical analysis was conducted using Graphpad Prism 7.0 statistics software and $P<0.05$ was considered to indicate a statistically significant difference. In the figures, asterisks denote statistical significance (*P <0.05, **P <0.01, ***P <0.001, ****P <0.0001).

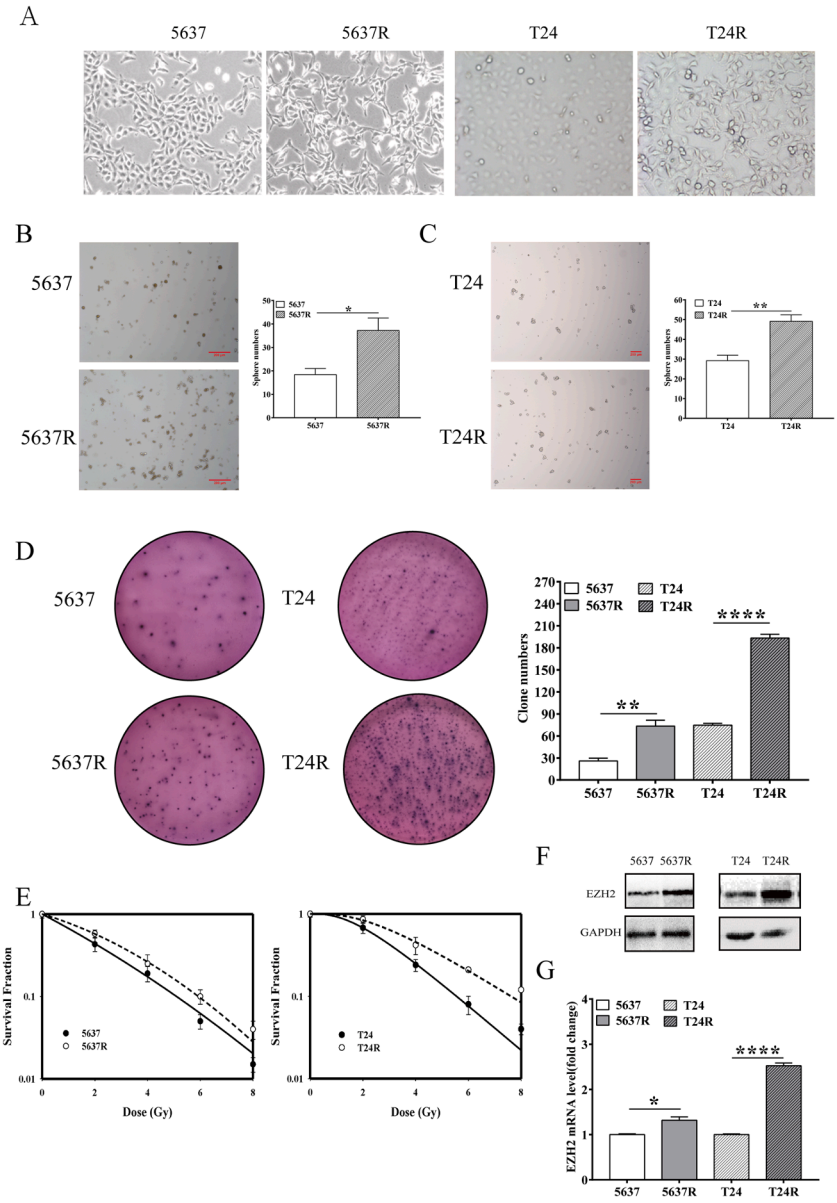

Fig. 1. ARR cells exhibit enhanced CSC properties and DNA damage repair ability.
(A) Representative images of morphology of 5637/ 5637R and T24/T24R under an inverted microscope (× 100). (B) CSC characteristics of 5637/5637R cells were detected by tumor microsphere culture. The representative images (B, left) and the quantification (B, right) were shown. Bar=200μm. (C) CSC characteristics of T24/T24R cells were detected by tumor microsphere culture. The representative images (C, left) and the quantification (C, right) were shown. Bar=200μm. (D) CSC characteristics of BCa cells were detected by soft agar colony anchoring assay. The representative images (D, left) and the quantification (D, right) were shown. (E) Cells response to γ-rays (0, 2, 4, 6 and 8Gy) was detected by CFA and surviving curve was fitted with Sigma Plot 11.0. (F) The expression of EZH2 in 5637/5637R and T24/T24R cells were detected by western blot. GADPH was loaded as an internal control. (G) The expression of EZH2 in 5637/5637R and T24/T24R cells were detected by qRT-PCR. *P < 0.05, **P< 0.01, ****P < 0.0001.

Results

FI enriched stem cell-like characteristics and increased EZH2 expression of BCa cells

In order to explore the mechanism of BCa recurrence and treatment tolerance after clinical radiotherapy, we established ARR cell model 5637R and T24R (Fig. 1A) by subjected human BCa cell lines 5637 and T24 to long-term IR as described previously [11]. With tumor microsphere culture and soft agar colony anchoring assay, we noticed that ARR cells (5637R & T24R) exhibited enhanced CSC properties compared to the parental cells (5637 & T24), respectively. The microsphere numbers of 5637 and 5637R were 18.40 ± 2.61 versus 37.20 ± 5.36 (P=0.034, Fig. 1B). Similarly, the microspheres of T24 and T24R were 29.20 ± 2.79 versus 49.20 ± 3.19 (P=0.009, Fig. 1C). The soft agar clones were 26.00 ± 3.61 vs. 73.30 ± 8.02 (5637 vs.5637R, P=0.006, Fig. 1D) and 74.67 ± 2.52 vs. 193.33 ± 5.13 (T24 vs. T24R, P<0.001, Fig. 1D), respectively. It should be mentioned that, compared with 5637 and 5637R cells, T24 and T24R cells can quickly form >50μM microspheres and visible colonies under the same conditions, which is consistent with the higher histological grade of T24 cells (III grade) than 5637 cells (II grade). On the other hand, accompanied by the tolerance to radiation (Fig. 1E), we noticed that the expression of EZH2 in ARR cell models was also significantly higher than that of the parental cells on both protein level (Fig. 1F) and mRNA (Fig. 1G).

High levels of EZH2 expression were associated with poor prognosis in patients with BCa

EZH2 is a popular target in the field of epigenetic anti-tumor research in recent years. Here, we made a bioinformatics analysis of its impact on the prognosis of BCa. Firstly, we compared the expression of mRNA of EZH2 in normal bladder tissue and BCa tissue samples based on the data from the Gene Expression Omnibus (GEO) and TCGA. Both NCBI GEO database (http://www.ncbi.nlm.nih.gov/geo/), GSE38264, GSE121711 and GSE37815) (Fig. S1A~C) and the Oncomine three database (Fig. S1D~F) showed that the mRNA expression of EZH2 was significantly higher in BCa tissues than that in normal tissues. Further subgroup analysis of 408 bladder carcinoma samples and 19 normal samples in the TCGA consistently supported that, compared to healthy people, BLCA patients exhibited a higher transcription of EZH2 based on gender, age, ethnicity, disease stages and tumor grade (Fig. S2). Next, using the GEPIA database, we evaluated the relationship between EZH2 mRNA expression and the prognosis of BCa patients. In the 201 cases included in GEPIA, the expression level of EZH2 mRNA was not significantly correlated with OS, but it was significantly negatively correlated with DFS (P=0.034), that is, DFS was lower in patients with higher expression of EZH2 mRNA (Fig. S3 A~B). In addition, based on the information of 405 BCa patients provided by Kaplan-Meier Plotter online database, we observed that although there were no significant differences in both OS and RFS between EZH2 high and EZH2 low patients, EZH2 ^{high} patients still exhibited a relatively low RFS rate to EZH2 ^{low} patients (Fig. S3C~D). Thus, we speculated that the expression of EZH2 may serve as a potential diagnostic indicator in BCa.

Down-regulation of EZH2 decreased the phenotype of radio-resistance and microsphere formation ability of BCa cells

To further investigate the role of EZH2 in BCa cells, we down regulated EZH2 expression by RNAi method (Fig. 2A). Both EZH2^{high} cells (5637 siCon&5637R siCon, T24 siCon&T24R siCon) and EZH2^{low} cells (5637 siEZH2&5637R siEZH2, T24 siEZH2&T24R siEZH2) were exposed to increasing doses of IR (0, 2, 4, 6 and 8 Gy) and cultured for obtaining stable clones. A dose-dependent reduction caused by radiation were observed in all lines. Moreover, all EZH2^{low} cells exhibited enhanced sensitivity to ionizing radiation compared to their EZH2^{high} counterparts. The surviving fraction at 2 Gy (SF_2) of 5637 siCon and 5637siEZH2 were 0.47 ± 0.04 and 0.42 ± 0.02 (P=0.359), respectively. For 5637R siCon and 5637R siEZH2 cells, the SF_2 were 0.83 ± 0.01 and 0.68 ± 0.02 (P=0.004), respectively. For T24 siCon vs. T24 siEZH2 and T24R siCon vs. T24R siEZH2 cells, the SF_2 were 0.79 ± 0.06 vs. 0.50 ± 0.01(P=0.009) and 0.90 ± 0.02 vs. 0. 80 ± 0.07(P=0.239), respectively

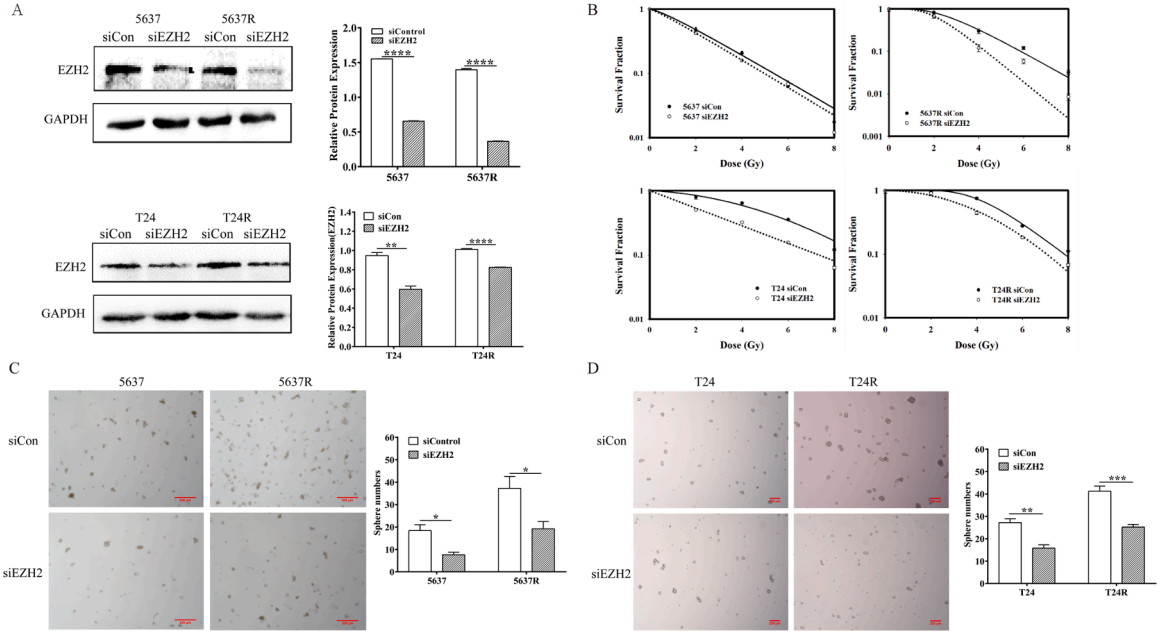

Fig. 2. Down-regulation of EZH2 decreased stem cell-like tumor cells and increased BCa cells radio-sensitivity. (A) The knockdown efficiency of EZH2 by RNAi were detected by Western blot. (B) The radiosensitivity of cells was detected by colony formation assay (CFA). Cells were exposed to increasing doses of IR (0, 2, 4, 6 and 8 Gy) and surviving curve was fitted with Sigma Plot 11.0. (C) Microspheres of 5637/5637R after knockdown EZH2 with RNAi were detected. The representative images (C, left) and the quantification (C, right) were shown. Bar=200μm. (D) Microspheres of T24/T24R after knockdown EZH2 with RNAi were detected. The representative images (D, left) and the quantification (D, right) were shown. Bar=200μm. *P< 0.05, **P < 0.01, ***P < 0.001, ****P < 0.0001.

(Fig. 2B). With the enhanced sensitivity to IR, the microsphere formation abilities of siEZH2 cells were significantly reduced compared to the control cells. 5637 siCon vs. 5637siEZH2, 18.40 ± 2.61 vs. 7.6 ± 1.14 (P=0.019), 5637R siCon vs. 5637RsiEZH2, 37.2 ± 5.36 vs. 19.20 ± 3.27 (P=0.046) (Fig. 2C); T24 siCon vs. T24 siEZH2, 27.20 ± 1.72 vs. 15.80 ± 1.47(P=0.00), T24R siCon vs. T24R siEZH2, 41.20 ± 2.32 vs. 25.20 ± 1.17(P=0.004) (Fig. 2D).

Down-regulation of EZH2 reduced DNA repair ability of BCa cells

Accumulation of the phosphorylated histone H2AX (γ-H2AX) on the sites of DNA lesions in the form of nuclear foci is one of the most established markers of DNA damage in response to irradiation. In current study, we exposed both parental cells and ARR cells to γ-ray of 2Gy and detected the formation of the γ-H2AX foci by immunofluorescence at different time points (2h, 12h, and 24h post IR), and un-irradiated cells as control. It was observed that, compared with parental cells, the foci of ARR cells decreased faster after irradiation (Fig. 3A, left), suggesting that ARR cells could have a stronger ability to repair radiation damage. In order to clearly compare the changes of DNA damage over time, we normalized the number of foci in 2 hours with the calculation formula: foci $_{(12h/24h)}$/foci$_{(2h)}$ × 100% (Fig. 3A, right & B) and the data was listed in Table S1(A: 5637 & 5637R; B: T24 & T24R). On the other hand, EZH2 knocking-down caused the numbers of γ-H2AX foci maintain a high level within 24 hrs post IR in BCa cells (Fig. 3C~D). It showed that there was no difference in the number of γ-H2AX foci in the cells of the control group and the EZH2 inhibition group 2h after the radiation. As time passed, the number of foci in the control group gradually decreased, while the number of foci in the EZH2 inhibition group remained relatively high. The high-level foci indicates that there is a large amount of DNA damage that has not been repaired. The normalization process is carried out with the number of foci in 0.5 hours, and the calculation formula is: foci ($_{2/6/12/24h)}$ / foci $_{(0.5h)}$ × 100%. The results were showed in Table S1C (5637 siCon & 5637 siEZH2), S1D (5637R siCon & 5637R siEZH2), S1E (T24 siCon & T24 siEZH2) and S1F (T24R siCon & T24R siEZH2).

Down-regulation of EZH2 affected the autophagic-flux stability of BCa cells

Autophagy, an intracellular conserved self-degradation system, plays a critical role in maintaining cellular homeostasis in response to external stimulus [12]. For BCa cells, EZH2-siRNA treatment significantly increased LC3BII/I ratio (Fig. 4A) and the proportion of LC3B-positive (Fig. 4B, top & C, left, Table S2A) of BCa cells, suggesting that autophagy was enhanced in those EZH2 down-regulated cells. We further detected the expression of P62 in the cells by immunofluorescence analysis. Compared to untreated cells, knocking-down EZH2 only increased the proportion of P62-positive cells in parental BCa cells (5637 & T24). However, EZH2 down-regulation did not affect the expression and distribution of P62 in radio-resistant cells (5637R & T24R) (Fig. 4B, bottom & C, right, Table S3A).

UNC1999, an EZH2 inhibitor, weakened the abilities of microsphere formation, DNA repair and autophagy regulation of BCa cells

In order to further observe the effect of EZH2 on BCa cells, a new S-adenosine-l-methionine competitive EZH2 inhibitor, was enrolled and untreated cells as control. Accompanied by the inhibition of EZH2 (Fig. 5A), the microsphere formation ability of BCa cells were significantly reduced, and the microsphere numbers of control and UNC1999-treated cells were 24.58 ± 2.05 and 18.00 ± 1.58 (5637, P=0.030), 45.60 ± 2.51 and 17.40 ± 3.36 (5637R, P<0.001), 26.20 ± 2.48 and 12.00 ± 2.10 (T24, P=0.012), and 46.40 ± 1.85 and 24.20 ± 3.54 (T24R, P=0.005), respectively (Fig. 5B). Also, pre-treated with UNC1999 caused the foci numbers of γ-H2AX maintained at a high level for a long time after BCa cells exposed to IR (Fig. 5C~D & Table S1 G~J) and increased the LC3BII/I ratio (Fig. 5E), the LC3B-positive proportion

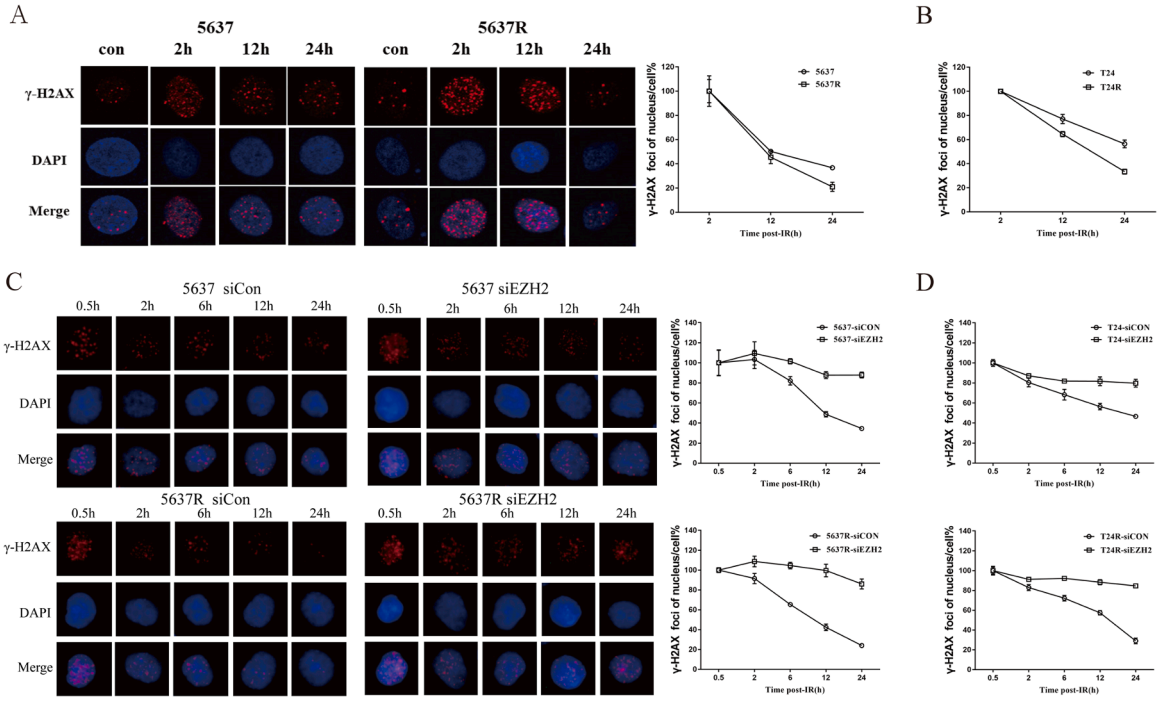

Fig. 3. Down-regulation of EZH2 weakened DNA repair ability of BCa cells. (A, B) DNA damage repair kinetics of cells was obtained by plotting the percentage of remaining foci against time. After irradiation with 2 Gy, 5637/5637R and T24/T24R cells were stained with γ-H2AX at the time point (2, 12, 24h) to determine remained foci formation. The calculation formula: foci numbers of 100 cells$_{(12h/24h)}$/foci numbers of 100 cells$_{(2h)}$ × 100%. (C, D) After irradiation with 2 Gy, cells with or without EZH2 transfecting were stained with γ-H2AX at the time point (0.5, 2, 6, 12, 24h) to determine remained foci formation. The calculation formula: foci numbers in 100 cells$_{(2/6//12/24h)}$/ foci numbers in 100 cells$_{(0.5h)}$ × 100%.

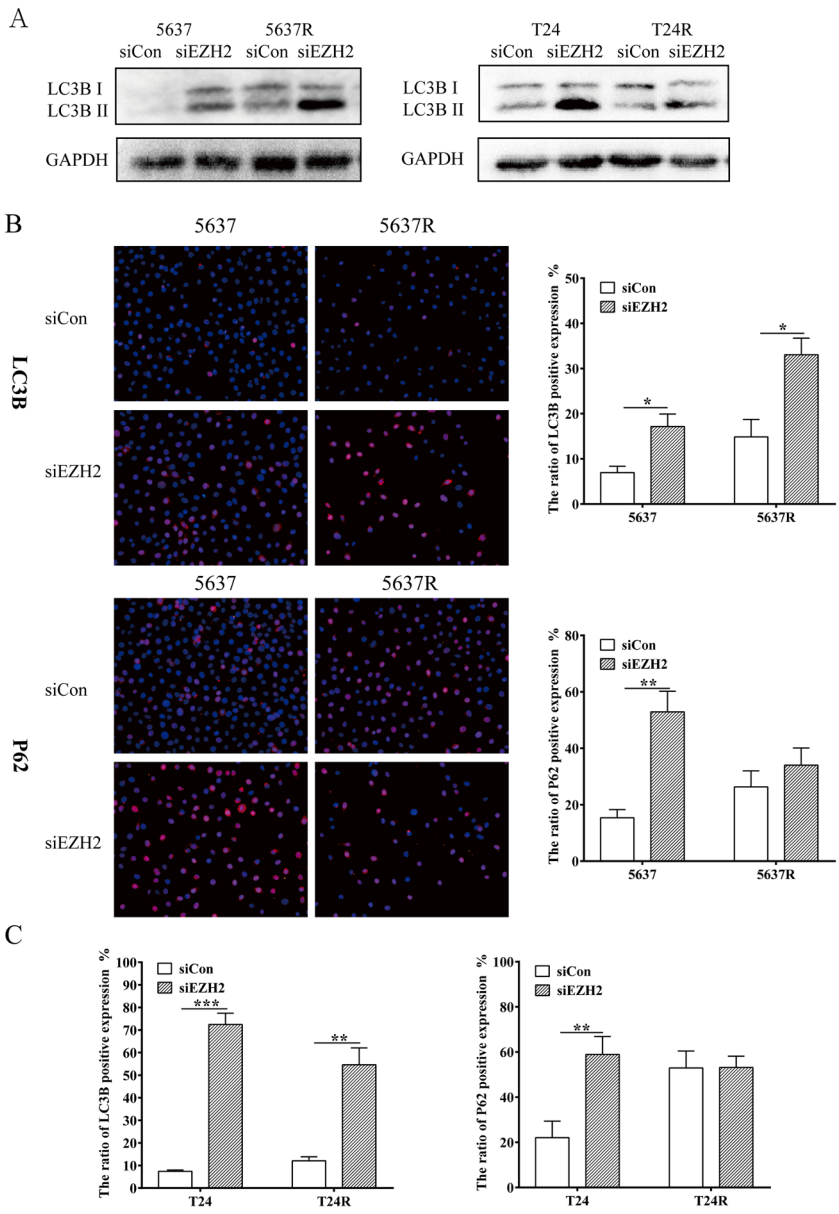

Fig. 4. Down-regulation of EZH2 affected the autophagic-flux stability of BCa cells . (A) The protein levels of LC3BI and LC3BII in cells transfected by siRNA were determined by Western blot. (B, C) The ratio of LC3B and P62 positive cells was detected by ICC. The calculation formula: positive cell numbers/total cell numbers in five independent fields × 100%. The representative images (B, left) and the quantification (B, right & C) were shown. Bar=50μm. *P < 0.05, **P < 0.01, ***P < 0.001.

(Fig. 5F, Table S2B) and the P62-positive proportion of BCa cells (Fig. 5G, Table S3B). We noticed that the ratio of P62(+) expression was raising in both UNC1999-treated parental cells and ARR cells. Whereas, EZH2 siRNA interference did not affect P62 expression in ARR cells (Fig. 4B&C).

Down-regulation of EZH2 restrained ARR cells growth in vivo

To demonstrate the effect of EZH2 inhibition on tumors, we employed mouse xenograft tumor models. Both parental BCa cells and ARR counterparts were injected to nude mice to observe the effect of EZH2-downregulation on tumor formation. However, only T24R cells formed tumors after inoculation in our experiments (Fig. 6A) [13]. It was found that untreated tumors took a period of 2 weeks (14 days) to reach around 800mm^3. During this period, treatment with UNC1999 (50 mg/kg, 3 times) alone (P=0.014, Day 14) or high dose of IR (4 Gy, 3 times) alone (P=0.0001, Day 14) started from 5 day suppressed the tumor growth, while combination treatment exhibited a robust inhibition of tumor growth compared to IR alone or UNC1999 alone (p<0.05, Day 14) (Fig. 6B) without body weight changes (Fig. 6C). At the endpoint of day14, tumor volume and tumor weight were, T24R Con: 779.78 ± 72.09 mm^3 and 0.82 ± 0.08 g, T24R UNC1999 alone: 517.05 ± 37.19 mm^3 and 0.38 ± 0.03g, T24R IR alone: 220.27 ± 39.21 mm^3 and 0.25 ± 0.03g, T24R UNC1999 + IR: 72.06 ± 39.90 mm^3 and 0.05 ± 0.02g, respectively (Fig. 6D), suggested that the combined treatment obtained a remarkable therapeutic efficacy.

On the other hand, due to lack of parental cells as a comparison, we herein introduced a human breast cancer cell line, MDA-MB-231 and its radio-resistant counterpart, MDA-MB-231R cells to perform in vivo experiments. Similarly, long term exposure to IR caused increased EZH2 expression in MDA-MB-231R cells, compared to MDA-MB-231 cells (Fig. 6E, left). Knocking down the expression of EZH2 (Fig. 6E, right), we observed that the tumor growth rate slowed down significantly (Fig. 6F). At the end of the experiment (Day 13), the tumor volume and tumor weight were measured and listed below, MDA-MB231 siCon vs. MDA-MB-231siEZH2, 560.59 ± 107.12 mm^3 vs. 199.58 ± 13.24 mm^3 (P=0.029), 0.25 ± 0.02 g vs. 0.10 g± 0.01 g (P<0.001); MDA-MB231R siCon vs. MDA-MB-231RsiEZH2, 696.33 ± 103.47 mm^3 vs. 371.19 ± 36.61 mm^3 (P=0.042); 0.25 ± 0.03g vs. 0.20 ± 0.01g (P=0.032), respectively (Fig. 6G). In comparison to control, down-regulation of

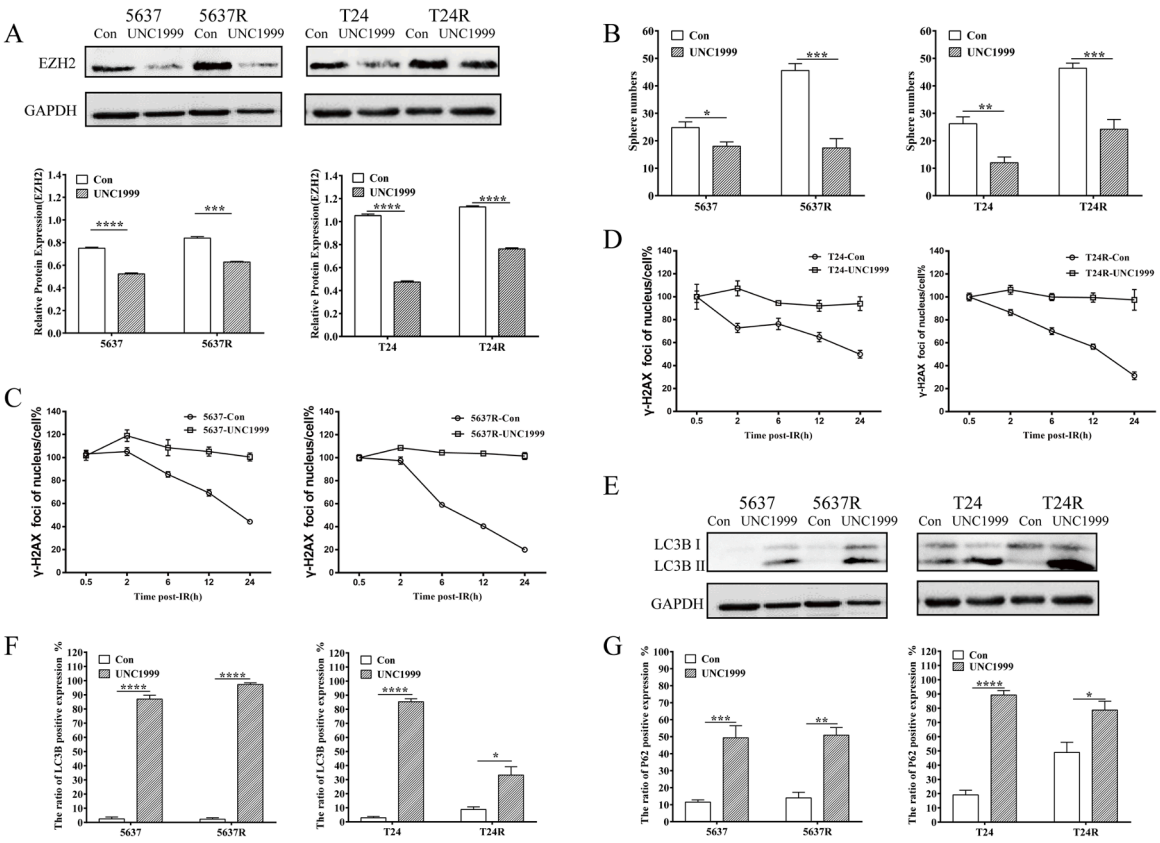

Fig. 5. UNC1999, a small EZH2 inhibiter, attenuated the abilities of microsphere formation, DNA damage repair and affected autophagy regulation of BCa cells. (A) The inhibition efficiency of EZH2 mediated by UNC1999 in cells were detected by Western blot. GADPH was loaded as an internal control. (B) Microspheres after inhibiting EZH2 with UNC1999 were detected. (C, D) DNA damage repair kinetics of cells was obtained by ICC. Cells with or without UNC1999 regulating were stained with γ-H2AX at the time point (0.5, 2, 6, 12, 24h) to determine remained foci formation. (E) The protein levels of LC3BI and LC3BII in cells treated by UNC1999 were determined by western blot. (F, G) The ratios of LC3B and P62 positive cells were detected by ICC. The calculation formula: positive cell numbers / total cell numbers in five independent fields × 100%. *P < 0.05, **P< 0.01, ***P < 0.001, ****P < 0.0001.

EZH2 expression greatly decreased the rate of tumor growth.

Discussion

BCa is one of the most common malignant tumors in the urinary system, accounting for approximately 90% to 95% of urothelial carcinoma [14]. The lifetime risk of BCa is approximately 1.1% in men and 0.27% in women [15]. On the other hand, age is the greatest risk factor for BCa, with an average age of diagnosis between 70 and 84 years [16]. These elderly patients are not appropriate for the basic therapy of cystectomy. Therefore, the bladder-sparing palliative therapies are commonly applied in the treatment of BCa, including radiotherapy, chemotherapy, immunotherapy, and close supportive medical care to alleviate symptom burden. Nowadays, high-precision 3D imaging guided radiotherapy greatly optimizes identification of the target volume sand surrounding at organs at risk (OARs) and minimize the side effects from dosing to other local organs [17]. Therefore, radiotherapy has been more and more widely used in BCa treatment. However, the occurrence of ARR phenomenon greatly reduces the effectiveness of radiotherapy. In order to find effective ways to overcome ARR, we first established ARR-BCa model by exposed parental cells (5637, T24) to FI of 2 Gy/day*30 times. The cells survived from long-term radiation and could be stably passaged are named 5637R and T24R, respectively. In addition to significantly decreased radiation sensitivity, both 5637R and T24R cells exhibited increased CSC properties, DNA damage repair abilities and EZH2 expression compared to 5637 and T24 (Fig. 1). Bioinformatics data analysis showed that EZH2, as an important biomolecule of epigenetic regulation, also played a major role in the occurrence and progression of tumors. It was found that BCa tissues have significantly up-regulated EZH2 mRNA levels compared with normal tissues in multiple datasets (Fig. S1) and in subgroup analyses based on gender, age, ethnicity, disease stages and tumor grade (Fig. S2). By analyzing the prognosis of BCa patients in the GEPIA databases, we observed that the DFS of $EZH2^{high}$ BCa patients was lower than that of $EZH2^{low}$ BCa patients (Fig. S3). Owing to the poor tumorigenicity of 5637 and T24, we failed to establish the corresponding tumor-bearing models, but T24R cells formed tumors after inoculation, suggested that ARR cells have a stronger degree of malignancy. With in vivo experiments, we noticed that combination treatment of EZH2 inhibitor UNC1999 and X-rays continuously suppressed the tumor growth. As a supplement, we enrolled a human breast cancer cell line, MDA-MB-231 and its ARR cells MDA-MB-231R to perform animal experiments in this study. As expected, knocking down EZH2 expression slowed down the growth rate of tumor tissues (Fig. 6).

Moreover, EZH2 is often overexpressed in many cancer types, especially in a variety of urinary system tumors [18, 19, 20] and positively correlated with poor clinical outcomes and metastatic disease [21,22], we believed that EZH2 should be an ideal tumor treatment target. Therefore, both RNA interference and small molecule inhibitor was applied to decrease EZH2 expression and methyltransferase function, respectively. It was noted that $EZH2^{low}$ cells are sensitive to radiation with weakened DNA damage repair ability and reduced microsphere forming rate compared to $EZH2^{high}$ cells (Figs. 2–5). In addition, we noticed that EZH2 inhibition induced autophagy by monitoring the ratio of LC3BII/I in BCa cells. It is known that autophagy is a dynamic, multi-step process involving the formation of autophagosomes, the

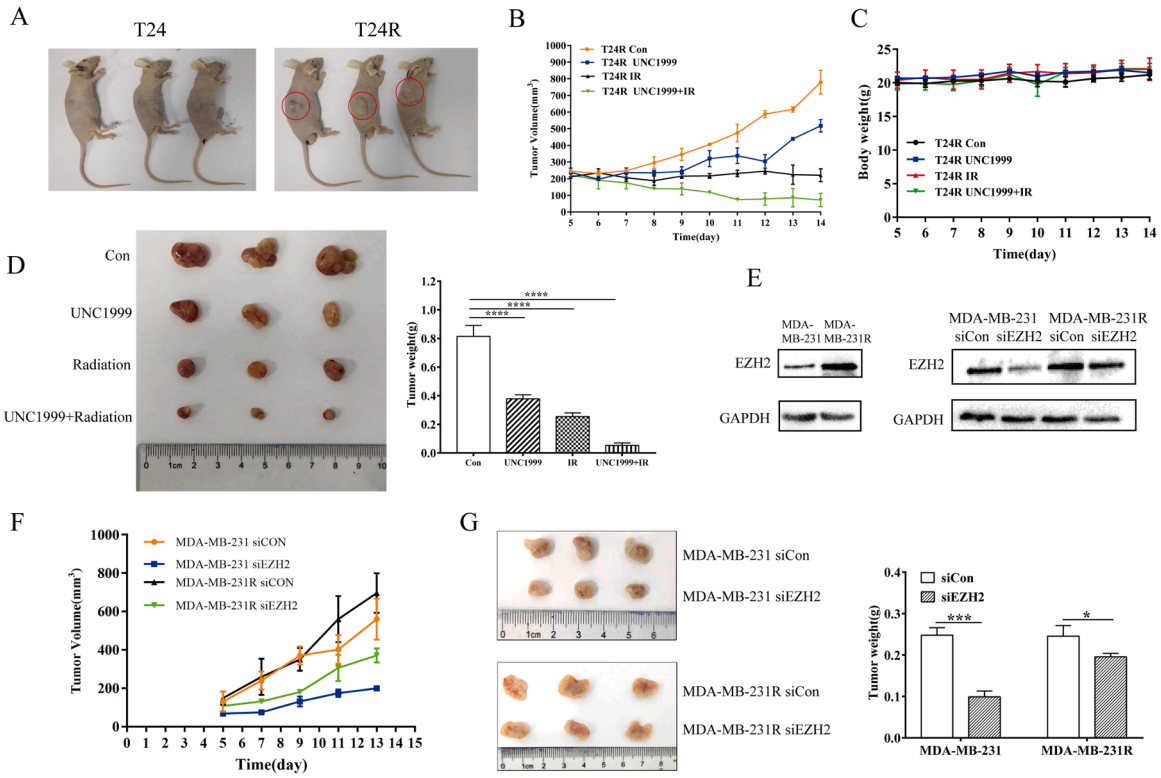

Fig. 6. Down-regulation of EZH2 restrained ARR cells growth in vivo. (A) Bladder cancer cells T24 and T24R (5×10^6) were injected into the right flank of nude mice, only T24R cells can form tumors. (B) T24R tumor volume was measured every day, from 5 days after injecting to 14 days. From the fifth day, mice bearing tumors were divided into 4 groups: T24R Con (without any treatment); T24R UNC1999(the inhibitor UNC1999 was injected into the tumor, 50mg/kg, every other day, 3 times in total); T24R IR (X-ray irradiation was carried out from day 6, 4Gy, every other day, 3 times in total); T24R UNC1999 + IR (at the same time of UNC1999 injection and irradiation). The calculation formula: $V=\pi \bullet L \bullet W^2/6$. (C) The body weight of mice were measured every day, from 5 days after injecting cells. (D) The images of T24R tumors obtained from sacrificed mice at the end of this experiment (Day 14) and the weight of tumor were compared. (E) The protein levels of EZH2 in MDA-MB-231 and MDA-MB-231R cells and knockdown efficiency of EZH2 by RNAi in cells were determined by western blot with GAPDH as internal control. (F) MDA-MB-231 tumor volume was measured every two days, from 5 days after injecting up to 13 days. The calculation formula: $V=\pi \bullet L \bullet W^2/6$. (G) The images of MDA-MB-231 and MDA-MB-231R tumors obtained from sacrificed mice at the end of this experiment (Day 13) and the weight of tumor were compared. *P $<$ 0.05, **P$<$ 0.01, ***P $<$ 0.001, ****P $<$ 0.0001.

fusion of autophagosomes and lysosomes to form autolysates, and the degradation of autolysates. Autophagosomes are autophagy markers with characteristic significance, which is used to evaluate the level of autophagy in cells [23]. Autophagosomes can be observed by electron microscopy, and can also be reflected indirectly by methods such as western blot detection of protein LC3BII [24]. Another widely used marker of autophagy flux is P62. Basic autophagy degrades P62 together with the target cargo by the lysosomal system, thereby maintaining the level of P62 at a relatively low level. The increase of LC3BII and P62 indicates that the autophagy flow is blocked and the maturation of autophagy is impaired, while the increase of LC3BII and the decrease of P62 indicate that the autophagy flow is activated and unobstructed [25]. In the current study, we found that autophagy-related protein changing after EZH2 siRNA transfection in ARR cells was inconsistent with that in sensitive cells (Fig. 4). P62 accumulation was only detected in siEZH-treated 5637 and T24 cells, not in 5637R and T24R cells upon the similar treatment. It suggested that in 5637&T24 cells, LC3B and P62 both increased after knocking down EZH2, indicating that the initial process of autophagy was activated, but the downstream did not work, phagosomes and lysosomes could not fuse or autophagy/lysosomal degradation pathways suppressed.While in 5637R&T24R cells, in response to EZH2 knocking down, the ratio of LC3BII to LC3BI increased more significantly, and the proportion of cells with positive expression of LC3B also increased dramatically, but the level of P62 did not change obviously. UNC1999, which decreased EZH2 expression and activation and caused LC3B and P62 accumulation in both parental cells and ARR cells, could be more effective to increase ARR cells responsiveness to treatment. However, Hsieh et al [26] reported that UNC1999 induced autophagy was partially dependent on ATG7 but independent of EZH2 inhibition. Therefore, we will continue to screen the best EZH2 targeted drugs to improve tumor cells, especially radiation tolerant cells, sensitivity to treatment.

In conclusion, EZH2 could be an important biomolecule linking the diagnosis, radiotherapy and prognosis of BCa. EZH2 targeted therapy may be an effective means to overcome ARR by reducing the DNA damage repair ability, stem cell characteristics and autophagy stability of BCa cells, and is worthy of in-depth study.

CRediT author statement

Xiangyan Zhang: Methodology, Investigation.
Xiangli Ma: Investigation,Writing- Original draft preparation.
Quanxin Wang: Data Curation.
Zhaolu Kong: Conceptualization,Writing - Review & Editing.

Declaration of Competing Interest

The authors declare that there are no conflicts of interest.

Authors' contributions

Zhaolu Kong designed the experiments. Xiangli Ma and Xiangyan Zhang performed the experiments. Xiangli Ma analyzed the data. Xiangli Ma and Zhaolu Kong wrote the manuscript.

Acknowledgments/Funding information

This work was supported by National Natural Science Foundation of China (grant no. 31870846).

Supplementary materials

Supplementary material associated with this article can be found, in the online version, at doi:10.1016/j.tranon.2021.101316.

References

[1] F. Bray, J. Ferlay, I. Soerjomataram, Global cancer statistics 2018: GLOBOCAN estimates of incidence and mortality worldwide for 36 cancers in 185 Countries. (2018).
[2] K. Saginala, A. Barsouk, J.S. Aluru, P. Rawla, S.A. Padala, A. Barsouk, Epidemiology of bladder cancer, Med. Sci. 8 (2020) 15.
[3] H. Sung, J. Ferlay, R.L. Siegel, M. Laversanne, I. Soerjomataram, A. Jemal, et al., Global cancer statistics 2020: GLOBOCAN estimates of incidence and mortality worldwide for 36 cancers in 185 countries, CA Cancer J. Clin. 71 (2021) 209–249.
[4] L. Silina, F. Maksut, I. Bernard-Pierrot, F. Radvanyi, G. Créhange, F. Mégnin-Chanet, et al., Review of experimental studies to improve radiotherapy response in bladder cancer: Comments and perspectives, Cancers 13 (2021) 87.
[5] Bladder cancer: diagnosis and management of bladder cancer, BJU Int. 120 (2017) 755–765.
[6] T. Shimura, S. Kakuda, Y. Ochiai, H. Nakagawa, Y. Kuwahara, et al., Acquired radioresistance of human tumor cells by DNA-PK/AKT/GSK3beta-mediated cyclin D1 overexpression, Oncogene 29 (2010) 4826–4837.
[7] S. Colak, J.P. Medema, Cancer stem cells–important players in tumor therapy resistance, FEBS J. 281 (2014) 4779–4791.
[8] J.A. Simon, C.A. Lange, Roles of the EZH2 histone methyltransferase in cancer epigenetics, Mutat. Res./Fundam. Molec. Mech. Mutagen. 647 (2008) 21–29.
[9] L. Shen, J. Cui, S. Liang, Y. Pang, P. Liu, Update of research on the role of EZH2 in cancer progression, Oncotargets Ther. 6 (2013) 321–324.
[10] T. Zhang, Y. Shen, Y. Chen, J. Hsieh, Z. Kong, The ATM inhibitor KU55933 sensitizes radioresistant bladder cancer cells with DAB2IP gene defect, Int. J. Radiat. Biol. 91 (2015) 368–378.
[11] G. Mao, Y. Yao, Z. Kong, Long term exposure to gammarays induces radioresistance and enhances the migration ability of bladder cancer cells, Mol. Med. Rep. 18 (2018) 5834–5840.
[12] A.V. Onorati, M. Dyczynski, R. Ojha, R.K. Amaravadi, Targeting autophagy in cancer, Cancer-Am. Cancer Soc. 124 (2018) 3307–3318.
[13] F. Wang, X. Ma, G. Mao, X. Zhang, Z. Kong, STAT3 enhances radiation-induced tumor migration, invasion and stem-like properties of bladder cancer, Mol. Med. Rep. 23 (2021) 87.
[14] A. Richters, K.K.H. Aben, L.A.L.M. Kiemeney, The global burden of urinary bladder cancer: an update, World J. Urol. 38 (2020) 1895–1904.
[15] P.M.L.K. Andrew, T. Lenis, Bladder cancer. A review, JAMA 324 (2020) 1980–1991.
[16] S.F. Shariat, J.P. Sfakianos, M.J. Droller, P.I. Karakiewicz, S. Meryn, B.H. Bochner, The effect of age and gender on bladder cancer: a critical review of the literature, BJU Int. 105 (2010) 300–308.
[17] S.E.M. Raby, P. Hoskin, A. Choudhury, The role of palliative radiotherapy in bladder cancer: a narrative review, Ann. Palliat. Med. 9 (2020) 4294–4299.
[18] X. Liu, Q. Wu, L. Li, Functional and therapeutic significance of EZH2 in urological cancers, Oncotarget 8 (2017) 38044–38055.
[19] L. Liu, Z. Xu, L. Zhong, H. Wang, S. Jiang, Q. Long, et al., Prognostic value of EZH2 expression and activity in renal cell carcinoma: a prospective study, PLoS One 8 (2013) e81484.
[20] M. Martínez-Fernández, C. Rubio, C. Segovia, F. López-Calderón, M. Dueñas, J. Paramio, EZH2 in bladder cancer, a promising therapeutic target, Int. J. Mol. Sci. 16 (2015) 27107–27132.
[21] J.I. Warrick, J.D. Raman, M. Kaag, T. Bruggeman, J. Cates, P. Clark, et al., Enhancer of zeste homolog 2 (EZH2) expression in bladder cancer, Urolog. Oncol. 34 (2016) 258, e1-258.e6.
[22] X. Zhang, Y. Zhang, X. Liu, T. Liu, P. Li, L. Du, et al., Nested quantitative PCR approach for urinary cell-free EZH2 mRNA and its potential clinical application in bladder cancer, Int. J. Cancer 139 (2016) 1830–1838.
[23] T. Noda, T. Kirisako, N. Mizushima, T. Ueno, T. Yoshimori, Y. Kabeya, et al., LC3, a mammalian homologue of yeast Apg8p, is localized in autophagosome membranes after processing, EMBO J. 19 (2000) 5720–5728.
[24] N. Mizushima, T. Yoshimori, B. Levine, Methods in mammalian autophagy research, Cell 140 (2010) 313–326.
[25] J. Moon, J. Jeong, J. Hong, J. Seol, S. Park, Inhibition of autophagy by captopril attenuates prion peptide-mediated neuronal apoptosis via AMPK activation, Mol. Neurobiol. 56 (2019) 4192–4202.
[26] Y. Hsieh, H. Lo, P. Yang, EZH2 inhibitors transcriptionally upregulate cytotoxic autophagy and cytoprotective unfolded protein response in human colorectal cancer cells, Am. J. Cancer Res. 6 (2016) 1661–1680.